GLOBAL BIOGEOCHEMICAL CYCLES, VOL. 15, NO. 3, PAGES 709–720, SEPTEMBER 2001

Methane oxidation in a peatland core

D. M. E. Pearce[1] and R. S. Clymo

School of Biological Sciences, Queen Mary, University of London, London, United Kingdom

Abstract. We made an experiment on a 30 cm diameter core of *Sphagnum*-dominated vegetation and peat to estimate the parameters controlling methane oxidation during movement to the ambient air: $^{13}CH_4$ was added at the water table, and excess $^{13}CO_2$ appeared in the gas space above the core. At 20°C in otherwise undisturbed conditions, ~22% of CH_4 was oxidized to CO_2 during passage up through the overlying 10-cm thick unsaturated peat and plants. We simulated the experiment, with seven parameters: transfer coefficients in water, in the gas phase, and through the container wall; the rate of CH_4 and of CO_2 generation; and the two parameters of a hyperbolic relation between CH_4 concentration and the rate of CH_4 oxidation. We optimized these parameters to fit the experimental results, and then were able to generalize to any temperature (0°–25°C) and any depth (0–55 cm) of water table. Changing temperature has important effects on the proportion of CH_4 oxidized.

1. Introduction

Peatlands cover ~3% of the Earth's land surface [*Clymo*, 1984]. About 3.5 million km^2, enough to form a square of side 1800 km, are in the Boreal zone [*Gorham*, 1991], especially in the former USSR, Fennoscandinavia, Canada, and the northern parts of the United States. The vegetation of much of this Boreal peatland is dominated by *Sphagnum* that, because it decays unusually slowly, comes to form a disproportionately large part of the peat [*Clymo*, 1984].

The surface layers of a peatland including the live plants and down to the depth to which the water table drops in a dry summer are collectively called the acrotelm [*Ingram*, 1978]. Below this is the peat proper: the permanently waterlogged and permanently anoxic catotelm, throughout which the hydraulic conductivity is relatively lower, by several orders of magnitude, than it is in the acrotelm. In the acrotelm the water table moves up and down as the balance among precipitation, evaporation, runoff, and downward percolation dictate, and the attendant transition from predominantly oxic conditions above the water table to anoxic ones below also moves up and down [*Clymo and Pearce*, 1995]. In this article the unsaturated zone is considered to be the acrotelm, and the saturated zone is considered to be the catotelm.

The surface of most Boreal peatlands is patterned on a scale of 1–10 m. Hummocks, from 10 to 60 cm tall, alternate with hollows, whose water table is above the surface in winter and below it in summer, and pools, whose water table is at the surface at all times. Each of these microforms has its own characteristic vegetation whose properties contribute to the maintenance of the microform [*Malmer et al.*, 1994]. Feedback mechanisms ensure the continued coexistence of hummocks and hollows [*Belyea and Clymo*, 1998].

At Ellergower Moss in southwest Scotland, a typical small rainwater-dependent raised bog, the concentration of CH_4 in the permanently waterlogged and anoxic catotelm increases approximately hyperbolically with depth [*Clymo and Pearce*, 1995]. This is consistent with continued slow production of CH_4 at all depths. The net upward flux can be inferred from the curve and is ~2% of the net efflux from the surface of hollows. Detailed measurements [*Daulat and Clymo*, 1998] show high peaks in CH_4 concentration profiles 10–15 cm below the water table. These peaks are barely a few centimeters thick and move up and down with the water table with a lag of only a few hours. The speed and size of these changes indicate that this is the main zone of CH_4 production. Diffusion and perhaps some mass flow carries the CH_4 upward to the atmosphere through peat, plant litter, and intercellular gas spaces in plants.

Overall, peatlands remove CO_2 from the atmosphere, sequester some of it as plant matter in peat [*Clymo*, 1984; *Clymo et al.*, 1998], and return most of it to the atmosphere as a result of decay. They also generate and emit CH_4, each molecule of which has (totalled over 100 years) ~20 times greater potential for climate change than the incoming CO_2 molecule from which it originated [*Houghton et al.*, 1996]. The net effect on climate of carbon sequestration and CH_4 emission varies with conditions and with the age of the peatland [*Alm*, 1997; *Clymo*, 1998; *Rivers et al.*, 1998]. It is not yet clear whether the effect is generally positive or negative, but there is no doubt that the net efflux of CH_4 must have a substantial influence, so any process that affects this efflux is important.

There have been numerous reports that the efflux of CH_4 from hollows is greater than it is from hummocks, beginning with *Clymo and Reddaway* [1971] and summarized by *Bartlett and Harriss* [1993] and *Crill et al.* [1993]. Almost as numerous have been the suggestions that this difference may result from CH_4 oxidation in the acrotelm of hummocks, though most of these reports could not exclude the possibility that the differences are a result of different rates of production. However, *Daulat and Clymo* [1998] found that in experiments in which the water table was moved, the profile of efflux in relation to water table was almost the same for hummocks as it was for hollows. This is better support for the oxidation hypothesis, though it is indirect.

Several authors have made experiments in which slurries, small pieces or cores of peat, soil, or sediment, were put in a closed container (in some cases with inhibitors of CH_4 oxidation such as CH_3F) and the disappearance of CH_4 from the gas phase or the appearance there of ^{14}C or ^{13}C or ^3H tracer in CO_2 was recorded [*Iversen et al.*, 1987; *Yavitt et al.*, 1988, 1990; *Whalen et al.*, 1990; *Whalen and Reeburgh*, 1990; *Reeburgh et al.*, 1991; *Whalen et al.*, 1991; *Crill*, 1991; *Whalen et al.*, 1992; *Sundh et al.*, 1992, 1993; *Crill et al.*, 1994; *Sundh et al.*, 1994; *Nedwell and Watson*, 1995; *Andersen et al.*, 1998; *Saarnio et al.*, 1998;

[1]Now at School of Biological and Molecular Sciences, Oxford Brookes University, Headington, Oxford, United Kingdom.

Paper number 2000GB001323.
0886-6236/01/2000GB001323$12.00

Gulledge and Schimel, 1998; *Brumme and Borken*, 1999]. Other workers have observed profiles of phospholipid fatty acids that are specific to methane-consuming bacteria [*Sundh et al.*, 1995], while *Fechner and Hemond* [1992] and *Reeburgh et al.* [1997] have inferred rates of oxidation from concentration profiles. *Reeburgh et al.* [1993] suggested that 30% of the CH_4 produced in high-latitude wetlands was oxidized before it reached the atmosphere.

It is clear from these works that the potential for CH_4 oxidation is widespread, but most of the observations have attendant difficulties too: they measure only potential or net potential, or they use inhibitors whose specificity may be uncertain [*Ormeland and Capone*, 1988], or the experiments were made in highly disturbed or far from natural conditions. One cannot extrapolate the results to different depths of acrotelm because they reveal little about the rates of those processes that contribute to the overall result: the rate of CH_4 production, the rate of transport, and the rate of oxidation. As far as we know nobody has yet tried to make direct measurements of the rate of CH_4 oxidation in minimally disturbed peatland conditions and to establish the values of parameters with which to assess the importance of CH_4 oxidation in peatlands in the wide range of conditions found in nature: a crucial element in the potential for climate change.

In this article we first describe measurements of the rate of CH_4 oxidation in a peatland mesocosm, using $^{13}CH_4$ as tracer. The experiment is expensive, so we then simulate it in a computer model and estimate the controlling parameter values so that the experimental results may be applied to other temperatures and other depths of acrotelm.

2. Materials and Methods

The principle of the experiment was simple. A 30 cm diameter core from the living surface of a peat bog, encompassing the acrotelm and the top of the catotelm, was put in a bucket on which a lid was sealed, enclosing some air above the surface of the core (the headspace). Water saturated with $^{13}CH_4$ and with unmetabolizable Kr as a physical tracer was injected at the water table. Samples of gas were then taken at intervals from the headspace, and the concentration of $^{13}CH_4$ and of $^{13}CO_2$ (and other gases) was measured with a mass spectrometer.

2.1. Experimental Cores

The peat core was taken from a hummock dominated by *Sphagnum capillifolium* with 5–10% cover of *Calluna vulgaris* shoots all less than 10 cm tall. It was one of a large series collected in northern Scotland [*Daulat and Clymo*, 1998]. An open-ended cylindrical stainless steel cutter, of 30 cm diameter and with sharpened sinuous teeth at the lower end, was pushed down with alternating rotation by ~30° to a depth of 50 cm. A wedge of peat was cut and removed from beside the cylinder to form a sloping ramp. A spade was forced through the peat below the bottom of the cutter and the cutter with core of vegetation and peat dragged out up the ramp and briefly laid horizontal while the core was cut at the bottom to 30 cm long. A bucket, 30 cm diameter, 40 cm tall, and made of 3 mm thick polyethylene, was laid horizontally so the cutter teeth fitted just inside its top. The cutter, core, and bucket were then stood upright, and the core slid slowly of its own accord into the bucket. The core in its bucket was taken to London and kept outside for about a year before the experiment was made. During this time the water table was maintained at a depth of 10 ± 1 cm below the top of the *Sphagnum* by automatically adding distilled water or allowing outflow from the core. For reasons explained in *Daulat and Clymo* [1998] we use "height" relative to the water table and "depth" relative to some other datum, usually the vegetation surface.

2.2. Experiments

Three preliminary experiments were made to establish suitable quantities and conditions. Here we describe their outcome in the design of the main experiment.

We needed a temperature that would encourage microbiological activity and that would not be far outside the normal range [*Daulat and Clymo*, 1998] for a peatland hummock, but we were not concerned about close control. The bucket and core were therefore taken to the mass spectrometer (MS) room, whose temperature varied in the range 18°–22°C: the mean summer temperature measured at 5, 10, and 20 cm deep in a hummock at Ellergower Moss in southwest Scotland was 12°–13°C [*Daulat and Clymo*, 1998]. The core was allowed to equilibrate for 24 hours before the experiment began. The bucket remained unmoved throughout the experiment.

About 500 cm^3 of equal parts of the gases $^{13}CH_4$ and Kr was shaken over 10% KOH to remove traces of CO_2. The Kr was to act as an unmetabolized marker of physical processes. The gas phase was transferred to another container holding 1050 cm^3 of distilled water that had been deoxygenated by boiling and had been allowed to cool to room temperature in a glass vessel with a water seal. The water and gases were shaken for 30 min to produce a saturated solution. This volume of solution was sufficient to occupy a layer 1.5 cm deep in the bucket. The same volume of water was removed from the core by siphoning, and the gas-saturated solution was injected laterally along a radial line in equal aliquots through six "Subaseal" bungs equally spaced around the height of the final water table. The water-saturated peat was then 20 cm thick; the unsaturated layer of peat, plant litter, and living plants through which CH_4 and Kr would have to move upward was 10 cm thick, and the headspace in which the gases would mix was also 10 cm thick. The bucket lid, which contained a vertical sampling port with lateral holes in the head space and a fan attached to the lower (internal) face, was then sealed on. The lid also contained a tube to a water-sealed U tube that allowed pressure inside and outside the bucket to remain the same ±0.3 cm head of water.

Before each headspace gas sampling, the fan was turned on, and the U tube outlet was blocked. A 5 cm^3 syringe was used to take a sample of the headspace gas. These 5 cm^3 samples were taken every 30 min for 8 hours on the first two days, every hour on the third day, once on the fourth day, and then at eight longer intervals up to the 52nd day giving, coincidentally, 52 samples. The lid remained sealed all this time. In the figures we describe the results to day 3 as "short term" and those to day 52 as "long term."

2.3. Subsidiary Experiments

Two subsidiary (control) experiments were made. In the first the main experiment was repeated with a sister core collected and stored in the same way as the one used in the main experiment but without the addition of Kr or $^{13}CH_4$. This experiment was a control intended to reveal any unanticipated isotopic fractionation of CH_4 and CO_2 during the long incubation.

In the second control experiment the bucket contained no vegetation or peat but was half filled with 14 dm^3 of freshly distilled water and (in the gas phase) nitrogen and traces of CH_4, excess $^{13}CH_4$, and CO_2. This experiment was to test the possibility that there might be exchange of ^{13}C between CH_4 and CO_2 or that CH_4 might oxidize in the absence of vegetation and peat. The surface of the water was at the same position in the bucket as the water table in the first two experiments.

2.4. Measurements on Gas Samples

The 5 cm^3 gas sample was allowed to expand into a partially evacuated glass bulb, and 10 subsamples were admitted, one after the other, to a Kratos MS50 RF magnetic sector mass spectrometer. The machine was set to allow automatic discrimination of mass/

charge (m/e) differences of 0.005 units, i.e., the ability to distinguish, for example, m/e 16.032 ($^{12}CH_4^+$) from 15.995 ($^{16}O^{16}O^{++}$). Each scan took ~2 min. In two cases, there were only nine scans, and in one case, there were only eight scans. The experiments reported here generated 1017 such scans with 14 clear peaks in most of them.

2.5. Numerical Treatments

The mass spectrometer scans were first calibrated for m/e on the two most widely spaced unambiguously identifiable m/e peaks. Usually these were 68.995 (internal $^{12}C^{19}F_3^+$) and 14.003 ($^{14}N^{14}N^{++}$). Special care was taken to separate the following peaks with m/e close to one another: $^{12}CH_4^+$ and $^{16}O^{16}O^{++}$; $^{13}CH_4^+$, $^{16}O^1H^+$, and $^{16}O^{18}O^{++}$; $^1H_2{}^{18}O^+$ and $^{40}Ar^{++}$. In some cases, however, a single real peak had been partially split by the machine into two or more, and these were recombined. Each peak was then expressed as a proportion of the total intensities in the scan. This allowed for small differences in subsample size. Finally, these proportions were converted using a separate standard to partial pressures. In the figures these partial pressures are given as ppm. We abstracted from the records the following species at the m/e given: $^{12}CH_4^+$ at 16.032, $^{13}CH_4^+$ at 17.035, $^{40}Ar^{++}$ at 19.981, $^{14}N^{15}N^+$ at 29.003, $^{16}O_2^+$ at 32.000, $^{12}C^{16}O_2^+$ at 43.990, $^{13}CO_2^+$ at 44.993, and $^{84}Kr^+$ at 83.912. Natural CH_4 and CO_2 both contain a proportion 0.0111 of ^{13}C. We were interested mainly in the fate of the extra ^{13}C we had added. In the figures we have therefore subtracted from measured $^{13}CH_4$ and $^{13}CO_2$ the amount calculated as coming from the simultaneously measured $^{12}CH_4$ and $^{12}CO_2$. We call the remainder "excess."

A measure of centrality and variation was then calculated for each m/e of interest for the (usually) 10 scans. The results contained ~10% of wildly erratic values, most of them only 1/10 or less of the mean of the other nine in the sample which had a coefficient of variation of ~0.05. We do not know the reason for these aberrant values, the mass spectrometer was 17 years old, but they are clearly distinct. Mean and standard deviation would have been strongly biased by these values, so we used the median and, as a measure of variability, the span of values containing 0.19 of the total observations below the median and the same value above the median. (This is like an interquartile range but with the bounds at 19% on either side of the median rather than at 25%.) If a sample distribution were Gaussian, then this span would be numerically the same as the standard deviation. We call this measure the G span and have plotted it on the figures. The calculation of proportioniles in general is described in appendix A.

In Figures 1–4, curves have been fitted using a self-adjusting simplex [*Nelder and Mead*, 1965]. In Figure 1b we use the negative exponential $y = y_m\, e^{(-at)}$, consistent with a decay process from initial maximum "y_m" at constant proportional rate "a," and $y = y_m\, e^{(-at)} + c$ consistent with a similar process but falling to a baseline "c." In all the others we use $y = y_m(1 - \exp^{(-at)})$ consistent with constant rate of addition "b" (where the asymptote $y_m = b/a$) as well as constant proportional rate of decay "a." We refer to these as "first-order flux equations," but the curves in Figures 1–4 are simply to aid the eye to judge whether such simple processes may be consistent with the observed kinetics.

3. Results

G-span range bars are shown in Figures 1–4. In many cases they are smaller than the size of the symbol marking the median. It is clear that "measurement error" is small and mostly smaller than "sampling error" (judged from deviations from trends), which is itself much smaller than the effects in which we are primarily interested. We therefore make no further comment on measurement or sampling error.

3.1. First Control Experiment

The experiment without the addition of Kr or $^{13}CH_4$ gave results very similar to the main experiment for $^{12}CH_4$, $^{12}CO_2$,

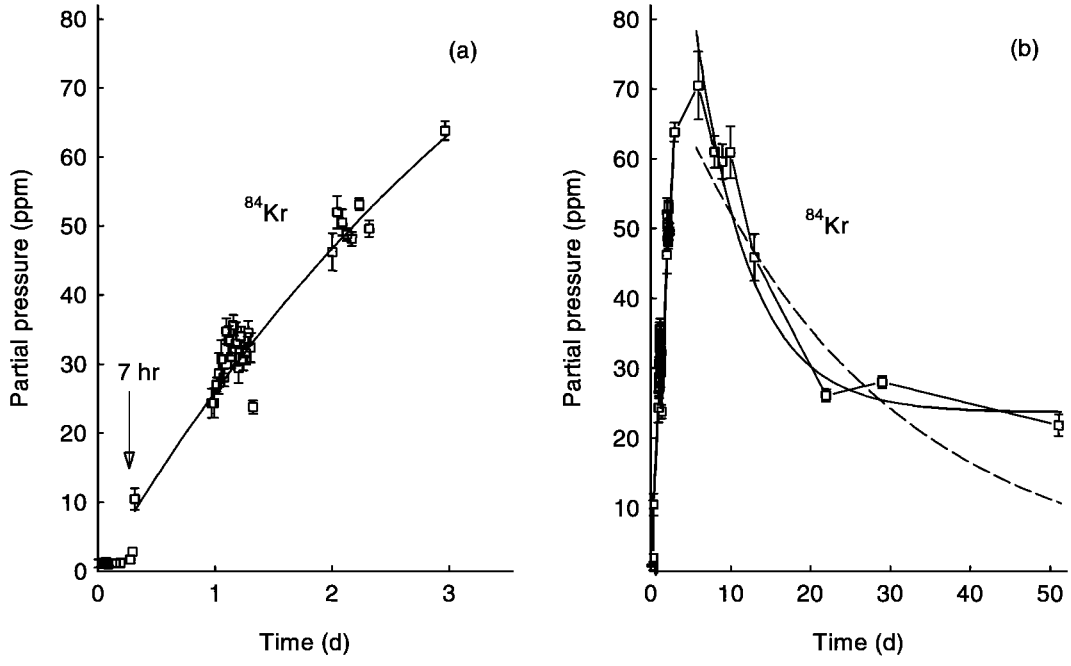

Figure 1. Time course of partial pressure of ^{84}Kr in the headspace over a hummock core. Values are medians; bars are ±1 G span (see appendix A). (a) Short-term (3 day) course. The curve (see text) is fitted to $y = y_m(1 - e^{-at})$. (b) Long-term (52 day) course. The dashed curve (see text) is fitted to $y = y_m\, e^{-at}$; the continuous curve is fitted to $y = y_m\, e^{-at} + c$.

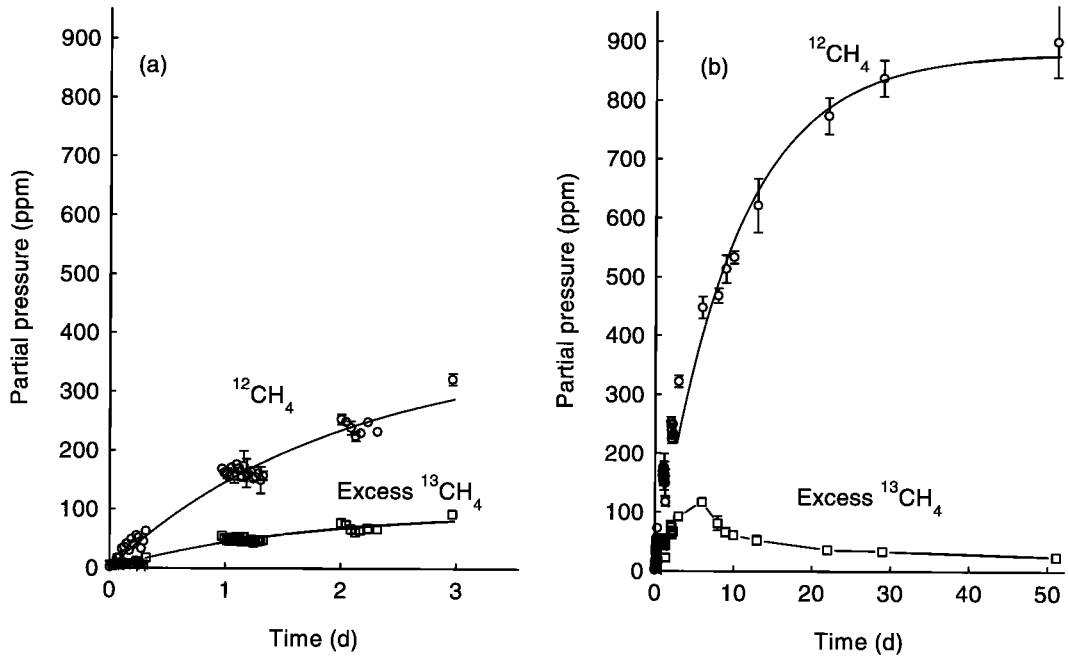

Figure 2. Time course of partial pressure of $^{12}CH_4$ and of "labelled" excess $^{13}CH_4$ in the headspace over a hummock core. "Excess" is the total minus that naturally present in the measured $^{12}CH_4$. Values are medians; bars are ±1 G span (see appendix A). (a) Short-term course. The curves (see text) are fitted to $y = y_m(1 - e^{-at})$. (b) Long-term course. The curve (see text) through the $^{12}CH_4$ points is fitted to $y = y_m(1 - e^{-at})$. For excess $^{13}CH_4$ the points are simply linked by straight lines.

$^{15}N^{14}N$, and ^{40}Ar. The quotient $^{13}C/^{12}C$ for both CH_4 and CO_2 was unchanged throughout the experiment, and that of CO_2 was close to natural abundance, indicating little change in microbial substrates or activities. The partial pressure of Kr, excess $^{13}CH_4$, and excess $^{13}CO_2$ were indistinguishable from zero (as expected).

3.2. Second Control Experiment

In the experiment (results not shown), in which the bucket was half filled by water and half by a mixture of nitrogen, traces of CH_4, excess $^{13}CH_4$, and CO_2, the partial pressures fell for the first 7 days toward a steady value: $^{12}CO_2$ fell to 50% of its starting value, while $^{12}CH_4$ fell much less to 96% of its starting value. At 20°C the solubility of CO_2 is 0.880 cm^3 cm^{-3}, while for CH_4 the value is 0.033 cm^3 cm^{-3}, ~1/25 as large. (Gas solubility coefficients are similar to partition coefficients not upper limits as they are for solids.) These coefficients applied to the gas and water volumes used would lead to partial pressures of $^{12}CO_2$ and $^{12}CH_4$ of 53% and 97% of the initial values, consistent with those observed.

The most important conclusion from this experiment is that in the absence of vegetation and peat, the rate of transfer of ^{13}C from CH_4 to CO_2 is very small: autooxidation or exchange can be ignored in the main experiment.

3.3. Main Experiment

When the lid was removed the *Calluna* plants, which had been in the dark for 52 days, were (not surprisingly) distinctly yellow. They and the *Sphagnum* did resume growth when returned outdoors. During the experiment the plants must have been respiring and thus have been a source of CO_2. The aboveground parts had a dry mass only ~1% of that of the unsaturated layer of peat, the main source of CO_2, so we ignore this complication. The concentration of O_2 fell steadily from the initial 20%: by day 22 it had fallen to 18%, and by day 52 it had fallen to 15%.

3.3.1. Physical behavior of Kr. Figure 1 shows results for the added Kr, which we hoped would behave physically in a similar way to the added $^{13}CH_4$ but without the complications introduced by biological interactions. The short-term behavior of Kr is shown in Figure 1a. (Natural Kr has several moderately abundant isotopes. They all behaved in the same way so we show ^{84}Kr only.) It took ~7 hours before extra Kr first appeared in the headspace. The partial pressure then jumped before settling to a steady, but slowly decreasing, rate of increase. The peak concentration was reached after ~7 days and then decreased for the next 40 days (Figure 1b). The dashed curve is fitted to a simple exponential decay, but the continuous one is fitted to exponential decay to a raised baseline.

There are several physical processes at work here. (1) In the short term, Kr diffuses upward from the water table through the unsaturated zone. Most of the movement must be in the gas phase, where the diffusion coefficient is much larger than it is in the interdigitating water. The process will, however, be modified by exchange between the gas and liquid phases. (2) Depletion in the water at the water table will slowly diminish the rate at which gas enters the unsaturated zone because it has first to diffuse from deeper down through water to the water table. (3) The headspace gas moves out slowly through the polyethylene container and possibly through small leaks around the edge of the lid. (4) Substantial amounts of CO_2 are produced in decomposition and raise the pressure in the headspace sufficiently to bubble out through the water seal, taking other gases with them. This would lead to an approximately negative exponential decline in concentration, as we observed. The kinetics of process 3 and 4 are not separable in the main experiment, but we note that in the subsidiary experiment there was no significant drop in gas concentrations after the initial solution changes. (5) Kr diffuses slowly down through the water in the peat below the layer to which it was added, and this decreases the concentration in the layer to which Kr was originally added, thus decreasing the rate at which it moves to the

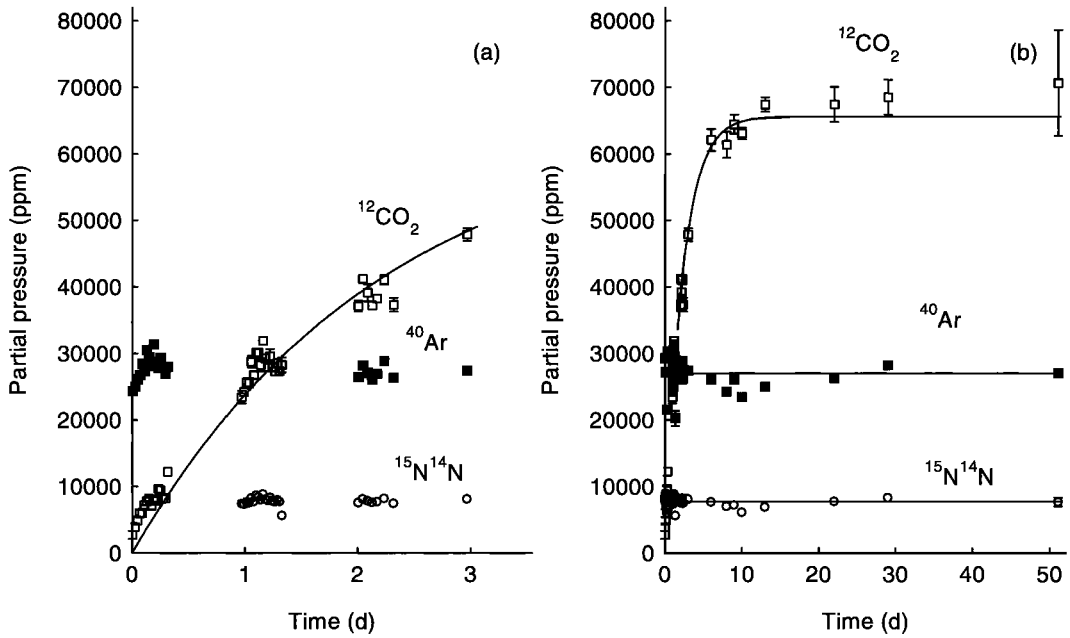

Figure 3. Time course of partial pressure of ^{40}Ar, $^{15}N^{14}N$ (m/e = 29), and of $^{12}CO_2$ in the headspace over a hummock core. Values are medians; bars are ±1 G span (see appendix A). (a) Short-term course. The first day's results for $^{15}N^{14}N$ and the second day's results for ^{40}Ar are omitted to avoid confusion with the $^{12}CO_2$ results. The curve (see text) is fitted to $y = y_m(1 - e^{-at})$ for all the results, not just the short-term ones. (b) Long-term course. The curve (see text) for $^{12}CO_2$ is fitted to $y = y_m(1 - e^{-at})$ for all the results. To the results for ^{40}Ar and $^{15}N^{14}N$, which were expected to be constant, straight lines were fitted. The slopes do not differ significantly from zero ($P < 0.01$).

headspace. Gas originally in a 1.5 cm thick layer becomes spread down through a 20 cm thick layer. However, because the solubility coefficient is only 0.067 cm^3 cm^{-3}, only ~5% of the remaining Kr is in the saturated zone, and the rest is in the unsaturated zone and headspace.

It is possible that the initial jump follows the establishment of the gas:liquid partition, as in process 1. The slowly diminishing rate of appearance in the first 7 days is consistent with a diminishing concentration at the water table (process 2) or the onset of loss through the headspace walls (process 3) and water seal (process 4), or a combination of these. The long-term exponential decline seen in Figure 3 may be dominated by losses through the walls (process 3) or (more plausibly) the water seal (process 4) and by diffusion downward into the saturated zone (process 5). However, the main conclusion must be that there are several processes at work here with consequences that can only be postulated. Later we simulate them. For the time being, the kinetics of Kr provide a descriptive background for those of $^{13}CH_4$.

3.3.2. Efflux of CH_4 and CO_2. Figure 2 shows the short-term and long-term results for excess $^{13}CH_4$. Its behavior is very similar to that of ^{84}Kr: an initial jump at 7 hours, a period to 7 days when the first-order flux equation is followed (Figure 1), and a much longer period during which there is a decline, in this case to ~1/5 of the peak value. The decline is proportionally greater than was that of Kr, and the difference may be a result of removal by oxidation to CO_2, though this evidence alone would be weak.

The behavior of $^{12}CH_4$ (also Figure 2) seems straightforward: it follows the first-order flux equation in both the short and long term, though the fitted efflux in the long term is only half that in the short term. We suppose the CH_4 is being produced by microbiological processes within the peat, and the efflux is the net efflux after any internal oxidation.

Figure 3 shows the short-term and long-term results for $^{12}CO_2$. The behavior is even simpler: the first-order flux equation is followed with the same parameter values throughout the experiment. Figure 3 also shows that as one would expect, the partial pressure of $^{15}N^{14}N$ (m/e = 29) and of ^{40}Ar changes little.

3.3.3. Oxidation of CH_4. The relation between all 52 measurements of the partial pressure of $^{12}CO_2$ (m/e = 44) and $^{13}CO_2$ (m/e = 45) is shown in Figure 4 for comparison with the line to be expected from the natural abundances of ^{12}C and ^{13}C. There is little doubt that there is an excess of $^{13}CO_2$. The excess ^{13}C is barely 10% of the total, but because the measurement error and sampling error (judged from the scatter about the trends) were both small, the main result shown in Figure 4b is clear: the excess $^{13}CO_2$ is ~90 ppm at a time, 7 days, when excess $^{13}CH_4$ is at a peak of 120 ppm. In terms of carbon, these concentrations are 22 and 78 ppm, so ~22% of the $^{13}CH_4$ has been oxidized to $^{13}CO_2$ during passage up through the unsaturated layer.

We have assumed that there is no microbiological discrimination between ^{12}C and ^{13}C in the production and oxidation of CH_4. This is untrue in detail, but the effect is relatively small.

4. Simulating the Experiment

4.1. Main Simulation and Parameter Optimization

The purpose of the simulation was to get best fit values of parameters, which could then be used to extend the applicability of the experiment. Details of the simulation are given in appendix B. It consists of a series of layers, 0.5 cm thick in the peat, different in the headspace and container walls. The initial concentration of the five measured substances (Kr, $^{12}CH_4$, $^{12}CO_2$, "excess" $^{13}CH_4$, and "excess" $^{13}CO_2$) is set in each layer, as are initial rates of the processes in each layer assumed to be governing transfer between adjacent layers. These assumptions required seven parameters: D_g, D_w, and D_c, the transfer coefficients of gases in the gas phase, in water, and in the walls of the container or through the water seal (cm^2 s^{-1}); P_M and P_C, the proportional rate of production on a dry

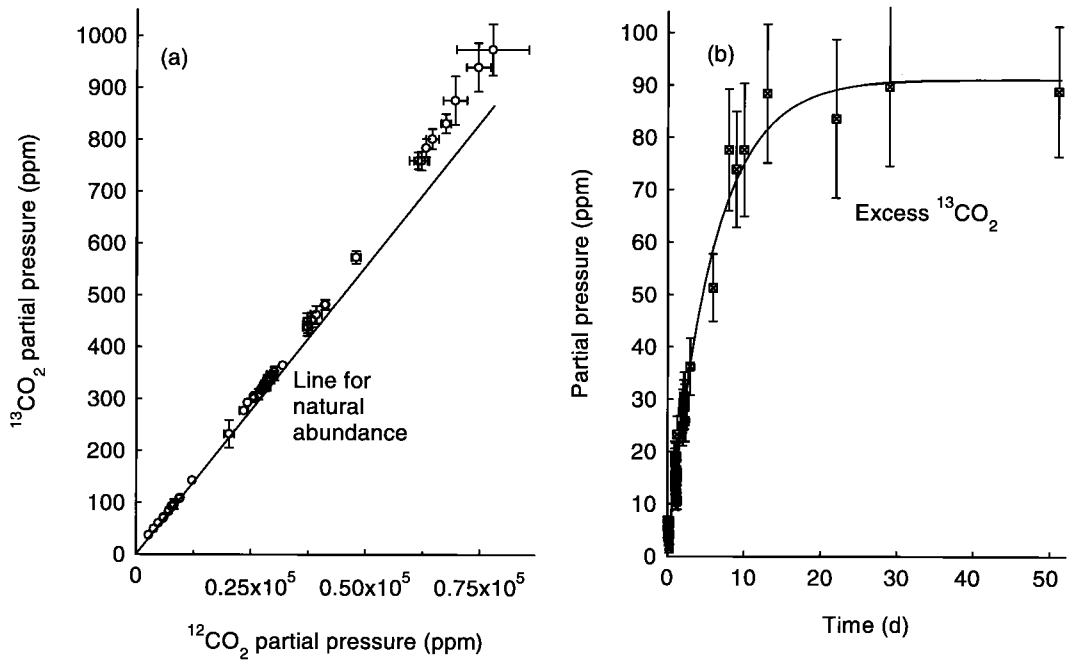

Figure 4. (a) Relation of partial pressure of $^{13}CO_2$ to that of $^{12}CO_2$ for the 52 samples of the headspace over a hummock core. Values are medians; bars are ±1 G span (see appendix A). The straight line is not fitted but is that expected for the natural abundance of $^{13}CO_2$ in the measured $^{12}CO_2$. At the highest partial pressures, equivalent to longest times, the excess of $^{13}CO_2$ is only ~10% of the natural abundance. (b) Time course of partial pressure of excess $^{13}CO_2$. The error bars include contributions from both $^{13}CO_2$ and $^{12}CO_2$ as both are involved in the calculation of excess $^{13}CO_2$. The curve (see text) is fitted to $y = y_m(1 - e^{-at})$.

mass basis of methane and carbon dioxide (yr^{-1}); and H_V (nmol s^{-1}) and H_K (nmol dm^{-3}), the maximum rate and the half-maximum concentration of a hyperbola relating CH_4 oxidation rate to CH_4 concentration in water. The last two are formally equivalent to V_{max} and K_m of Michaelis-Menten enzyme kinetics, but we do not imply that we are studying a simple enzyme reaction in a well-stirred solution.

All the amounts to be transferred are calculated from the present concentrations and rates. Only after all the amounts have been calculated are the transfers effected giving new concentrations in each layer. New rates (which depend on the new concentrations) are now calculated. This completes one iteration. Typically, the model time increment was ~10–15 s. The process was then iterated some 100,000 times to cover the first 13 days of the experimental data (it was infeasible to run the model regularly to the full 52 day data set). This gave a series of concentrations of the five variables in the headspace that were compared with those measured, to give a criterion measuring the badness of fit. Such a "run" produced a single value of the criterion. An optimization technique used multiple runs to get a set of parameter values that minimized the criterion. By that time the model had been evaluated several tens of millions of times.

After the difficulties described in appendix B had been overcome, the simulation proved well behaved. The best fit of the five gases in the headspace is shown in Figure 5. The concentration (y axis) scale is logarithmic to cover the range of concentrations, and this misleadingly emphasizes poorness of fit at low concentrations. The parameter values for the best fit are shown in Table 1. It was not feasible to estimate the variance of these values, but some indication can be had from the relative sensitivities, which are the proportional rate of change of the criterion for a common proportional change in the parameter value. Thus D_c with a large sensitivity is rather exactly determined, while P_M is inexact.

Concentration profiles in the model are shown in Figure 6. These are much as expected, with large peaks in CH_4 concentration below the water table, similar to those observed by *Daulat and Clymo* [1998].

4.2. Extension of the Simulation

Finally, we modified the model to simulate different temperatures and thicknesses of the unsaturated layer but kept the best fit parameter values. The relation between diffusion rate of gases in water and temperature in the range 0°–25°C is exponential [*Briggs et al.*, 1961] with an increase of 0.02°C^{-1} equivalent to a Q_{10} of 1.2.

The relation between rate of CH_4 and CO_2 production and temperature is also exponential [e.g., *Dunfield et al.*, 1993; *Daulat and Clymo*, 1998; *Nedwell and Watson*, 1995] with Q_{10} values from 4 to 6 with isolated values as high as 16. For the simulation we used Q_{10} of 5.0, equivalent to an exponent of 0.16°C^{-1}.

The relation between CH_4 oxidation rate and temperature is less clear. *King and Adamsen* [1992] working on 6 cm diameter cores of soil from a mixed deciduous and conifer forest found [*King and Adamsen*, 1992, Figure 2] no consistent effect of temperature in the range 0°–30°C (but summarize these results by rate constant = $aT^{2.4}$, which seems implausible). *Crill* [1991], working on similar samples with similar techniques, also found little effect of temperature in the range 5°–27°C. However, other authors report larger effects. *Whalen et al.* [1990, Figure 5b] used 7 cm diameter cores from soil covering landfill, and *Dunfield et al.* [1993, Figure 4] used peat slurries. Both showed rates of CH_4 oxidation near zero at temperatures below 5°C and ~1–5 μmol cm^{-3} d^{-1} (converted to a volume basis) at 25°C. Both report a Q_{10}: 1.9 and 1.4–2.1,

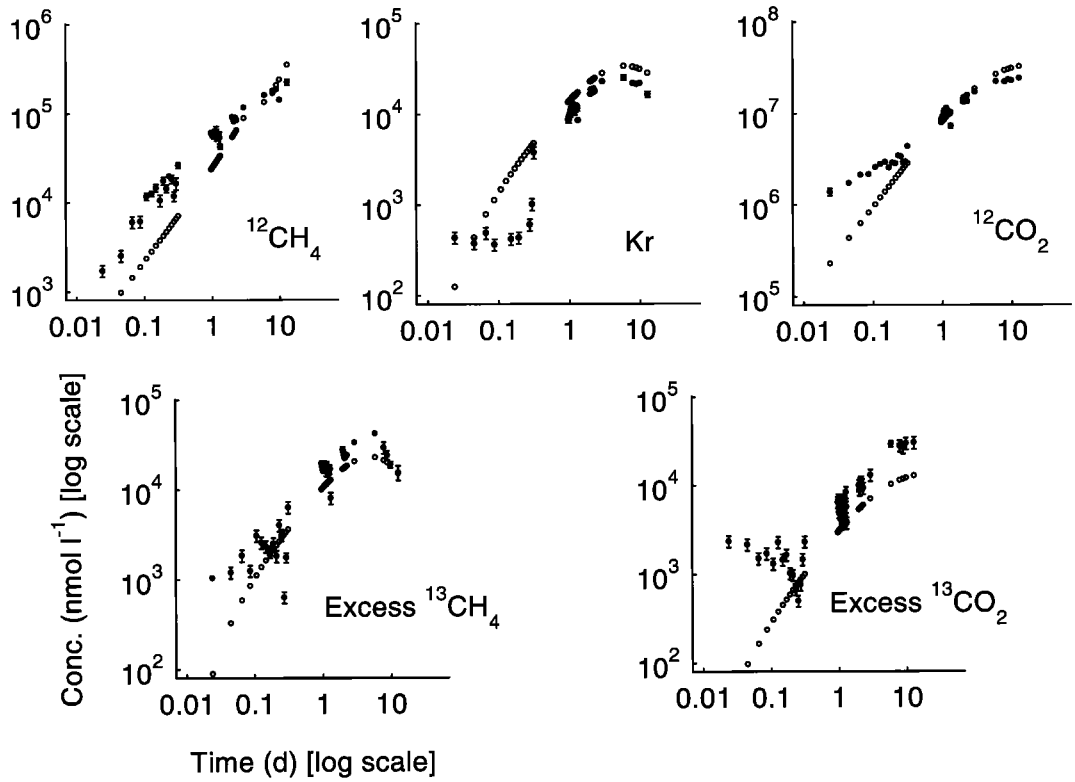

Figure 5. Time course of measured (filled symbols with ±1 G span bars) and modeled (open symbols) concentrations of five gases in the headspace, using the best fit of seven parameters (see text and appendix B). Both axes are scaled logarithmically spanning 3 orders of magnitude, to accommodate the long times and big differences in concentration. This causes deviations at low concentrations to be unduly prominent.

respectively. Finally, *Nedwell and Watson* [1995], using peat slurries, report a good fit to an Arrhenius plot and a Q_{10} of 2.2 but show no data. We note that this range of absolute temperature (273°–298°K) is so small that many functional relationships would appear to be a good fit on an Arrhenius plot. One may doubt the validity and use of "activation energy" derived from such plots of complex systems, but even the concept of a Q_{10} implies an exponential relationship, with a nonzero intercept at 0°C. *Whalen et al.* [1990, Figure 5b] and *Dunfield et al.* [1993, Figure 4] are better fitted by a linear relation with very small or zero intercept at 0°C than they are by an exponential one. For the simulation therefore we have assumed a linear relationship between oxidation rate and Celsius temperature, with zero intercept at 0°C.

Figure 7 shows the results of 66 such simulations. For a hummock of height 30 cm and temperature 10°C, the simulation suggests that ~40% of the CH_4 would be oxidized before reaching the atmosphere. A 50% error in the temperature exponent for diffusion produces a slightly greater proportion oxidized at 5°C but a very slightly decreased proportion at 25°C. The proportion oxidized is in direct proportion to an error in the oxidation rate, and (not shown) errors in the rate of CH_4 and CO_2 (decay) have almost no effect on the proportion oxidized, though they do of course affect the efflux of these gases.

Table 1. Parameter Values and Relative Sensitivities for the "Best Fit" (Minimum) Criterion Value

Parameter Symbol	Name	Units	Value	Relative Sensitivity[c]
D_g	Transfer coefficient of gas in the gas phase	cm^2 s^{-1}	2.0	2.0
D_w	Transfer coefficient of gas in water	cm^2 s^{-1}	6.5e-6[b]	1.3
D_c	Transfer coefficient of gas in the container wall[a]	cm^2 s^{-1}	0.032	3.0
P_M	Proportional rate of CH_4 generation	yr^{-1}	0.50	−0.7
P_C	Proportional rate of CO_2 generation	yr^{-1}	0.25	4.0
H_V	Maximum rate of oxidation of CH_4 to CO_2	nmol s^{-1}	0.01	0.5
H_K	Concentration for half-maximum rate of oxidation	nmol dm^{-3}	2.1	−1.8

[a] Includes transfer through the polyethylene and the more significant escape through the water trap.

[b] Read 6.5e-6 as 6.5×10^{-6}.

[c] Proportional change in the optimization criterion when the parameter value is changed by 5%, expressed as $\log_{10}$. Larger is more sensitive.

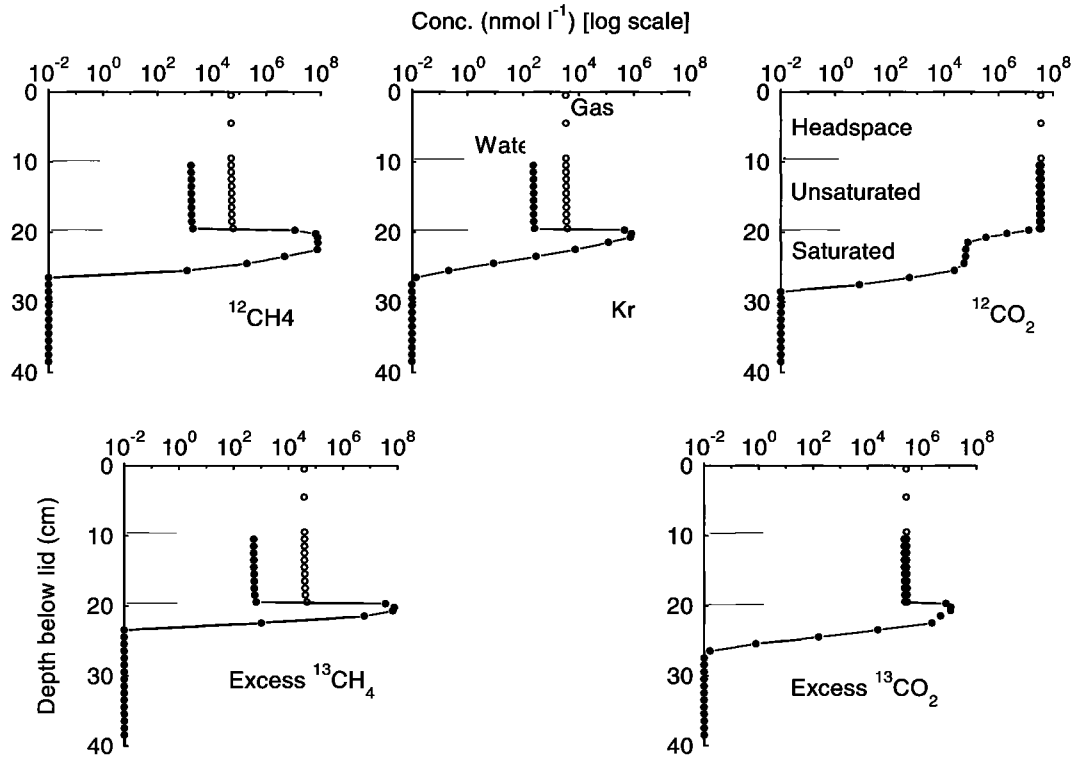

Figure 6. Concentration profiles of five gases in water (filled symbols) and in the gas phase (open symbols) in the model after 13 days, using the best fit of seven parameters (see appendix A). There is no water phase in the headspace and no gas phase in the saturated layer. The concentration axis is scaled logarithmically.

After 7 days, when the concentration of $^{13}CH_4$ in the headspace was at its maximum (Figure 2), 2.0% of the added ^{13}C was in CH_4 in the headspace, 23.6% was in CH_4 in the water in the unsaturated layers, 1.2% was in the gas phase of the unsaturated layers, and 64.8% was still in the saturated layers where it had been added. Already oxidized to CO_2 was 0.9% in the headspace and 2.0% in the unsaturated layers. About 5.3% had escaped from the system.

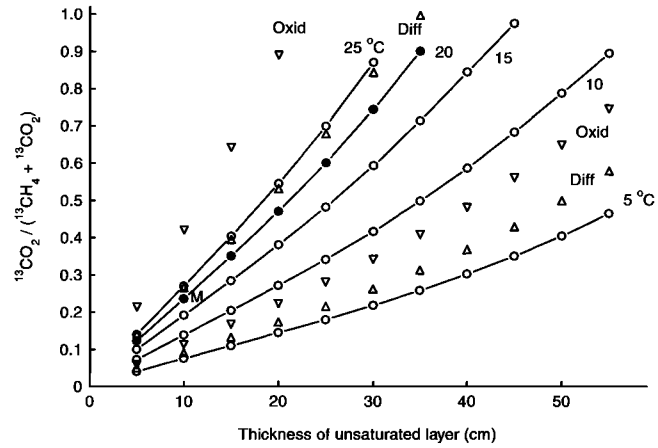

Figure 7. Calculated proportion that $^{13}CO_2$ forms of total ^{13}C in the headspace (=proportion of CH_4 oxidized) in relation to thickness of the unsaturated layer and of temperature (see text). The points connected by lines use temperature exponent of diffusion = $0.02°C^{-1}$ (Q_{10} = 1.2), of gas production = $0.16°C^{-1}$ (Q_{10} = 5), and oxidation versus temperature slope multiplier = 1.0. Sensitivity for diffusion is shown by upward pointing triangles for exponent = $0.03°C^{-1}$ (Q_{10} = 1.4) at 5° and 25°C; sensitivity for oxidation by downward pointing triangles with factor = 1.5 at the same two temperatures. "M" indicates the point established from the experiments. All the other points are inferred from the model. At 0°C, all values are zero; these and unphysical values >1.0 are omitted.

5. Discussion

5.1. Main Experiment

The main result of this experiment is that at ~20°C, 22% of the added $^{13}CH_4$ was oxidized to $^{13}CO_2$ on its way up through the 10 cm of unsaturated *Sphagnum* to the headspace. The experiment was made with an intact system that was actively growing for a year before the experiment and resumed growth after it. The system preserved the microbial and fungal communities and the natural physical juxtapositions of organisms and materials. However, it is widely believed that part at least of the CH_4 in peatlands is produced from simple carbohydrates secreted from active roots [e.g., *Chanton et al.*, 1995] and the plants were in the dark during the experiment. It is also true that the temperature of the experiment was ~10°C higher than would be common in the field and that the water table was static. Yet the measured net efflux of CH_4 fitted to the results in Figure 2b was 280 μmol m^{-2} hr^{-1}, while in the field the efflux from a 10 cm hummock with temperature at 10 cm depth of 14°C was 115 μmol m^{-2} hr^{-1} [*Clymo and Pearce*, 1995]. This difference is almost exactly that calculable from the exponential effect of temperature on net efflux of CH_4 [*Daulat and Clymo*, 1998] from cores similar to those used in this experiment, which in any case contained only 5–10% by area of vascular plants, the rest being *Sphagnum*—covered. We also note that the water table in raised peatlands is within 2.5 cm of the mean height for nearly 70% of the time. These results are consistent with the view that the experimental core behaved much as one in natural conditions would do.

5.2. Simulation

The best fit parameter values for the simulation (Table 1) were determined with widely differing sensitivity. The transfer coefficients of gases in the gas phase and in water (D_g, 0.8; D_w, 6.4 × 10^{-6} cm^2 s^{-1}) are not dissimilar to the accepted values of the molecular diffusion coefficients obtained by direct measurement (0.2 and 1.2 × 10^{-5} cm^{-2} s^{-1}) and to the 0.6 cm^{-2} s^{-1} inferred for C_3H_8 in the unsaturated top 7 cm of a peatland by *Fechner and Hemond* [1992]. The transfer coefficient of the container wall (D_c, 0.032 cm^2 s^{-1}) is several orders of magnitude greater than the diffusion coefficient of gases through polythene, but the model also shows that 18% of the Kr and 19% of the ^{13}C have disappeared from the system after 13 days. These features are consistent with the suggestion that pressure driven escape of gases through the water seal is causing the headspace to behave like a dilution vessel. The gas production (peat decay) coefficients (P_M, 0.50 yr^{-1} and P_C, 0.25 yr^{-1}) seem plausible at the mean temperature of 20°C: they seem to indicate that anaerobic CH_4 production is, within its thin zone, an even more effective decay process than aerobic CO_2 production, a conclusion consistent with the findings of *Belyea* [1996]. However, we note that P_M is imprecisely determined.

The CH_4 oxidation parameter values were H_V = 0.6 nmol s^{-1} and H_K = 2.1 nmol dm^{-3}, but both were imprecisely determined, the latter being the most insensitive of all the parameters. The hyperbolic definition of the oxidation process was formally identical to that of an enzyme reaction. However, Michaelis-Menten kinetics assume a well-stirred solution and relatively simple chemistry, while our experiment and natural conditions in peat are unstirred and complex. We think that the dynamics of oxidation are probably much more affected by the rate of diffusion of substrates and products than by the properties of the enzymes involved, and the insensitivity of determination of these oxidation parameters reflects this: a wide range of values produces almost as good a fit because the factory is limited by transport to and from it not by its machinery and internal organization. *Conrad* [1996] reviewed the ways in which soil microorganisms may control atmospheric trace gases but did not consider the role of diffusion. Yet this is not a new idea: much of the early work on uptake of solutes by plants was shown [*Olsen*, 1953a, 1953b; *Bircumshaw and Riddiford*, 1952; *Briggs et al.*, 1961] to be studying diffusion rather than the biochemical processes the authors intended.

The experiment was made in a closed container with minimal mass flow of air. In the field, one would expect wind-induced mixing in the unsaturated zone to be greater than in the experiment. We therefore tried the effect of increasing the value of D_g by a factor of 10. The results were little affected. This is not a good representation of turbulent flow, but we recall that the spaces between structural elements in the unsaturated zone are no bigger than a few millimeters, and turbulent mixing is probably small anyway.

5.3. Wider Application

The values in Figure 7 have been extrapolated from a single measurement at 20°C with the water table at 10 cm depth: caution is necessary. In the field the net efflux from 40 cm high hummocks at a mean summer temperature of 14°C was 40% of that from hollows [*Clymo and Pearce*, 1995] implying, if one accepts that the production rate beneath both is the same [*Daulat and Clymo*, 1998], that 60% had been oxidized. Figure 7 suggests 50% is oxidized. In the circumstances this seems to be a reasonable agreement. *Reeburgh et al.* [1993] suggested that 30% of the CH_4 produced in high-latitude wetlands was oxidized before emerging into the atmosphere: close to the value in Figure 7 for 20 cm hummocks at a summer temperature of 10°C.

Can these effects be applied on a larger scale? Suppose that the mean temperature 10°C and that the acrotelm (unsaturated layer) depth is 30 cm. Suppose also that the CH_4 production in a given time is 100 units, oxidation (Figure 7) is 0.42 × 100 = 42 units, giving net efflux of 58 units. Now increase the temperature by 1° to 11°C. Production (Q_{10} = 4) would increase by 50% to 150 units, oxidation becomes 0.45 × 150 = 68 units, and net efflux is 82: an increase of 24 units but less than half the 50 units it would have been without oxidation. Because production has an exponential response to temperature but the oxidation response seems to be near linear (or at least, if exponential, has a much smaller exponent than production does), any increase in temperature will produce some increase in efflux. If, however, in the example above, the change of temperature was accompanied by a drop in water table of 10 cm, then the increases in oxidation caused by higher temperature and deeper unsaturated zone would result in no overall change in efflux.

These calculations are quite sensitive to the depth of the unsaturated zone and to the mean temperature. We do not know the distribution of depth of the unsaturated zone for even a single small peatland, nor do we have better than a vague idea of how that distribution might change over 10–50 years in response to a step change in precipitation. For these reasons it is unhelpful, if not misleading, to try to apply the results of this experiment to the global scale at present. This sort of calculation also ignores possibilities such as Northern Hemisphere peatlands at the southern end of their range disappearing altogether, while new ones form in the north.

Before we began this work, it was widely assumed that CH_4 was oxidized during passage up through peatland hummocks, but most of the evidence was indirect and qualitative only. We now have direct evidence of the process and can calculate, tentatively, the proportion of CH_4 oxidized to CO_2 at realistic temperatures and depths of acrotelm.

Appendix A: G Span Variability Measure

For reasons given earlier, we needed to calculate proportioniles (quantiles), i.e., that value of the measured variable, which includes

a specified proportion of the sample or population. Statistics textbooks deal with this, usually for the 25 and 75% cases needed for the interquartile range, but they use a surprising number of nonequivalent recipes to do this. We devised the following.

Let n be the number in the sample or population. Let p be the proportionile required, where $[1/(2n)] < [p] < [1 - 1/(2n)]$. (For the median, $p = 0.5$; for the interquartile range, $p = 0.25$ and 0.75.) Let a be trunc(np), and $\underline{a}$ be the value of the ath member of the sample or population when it has been arranged in ascending order from $a = 1$. We use linear interpolation between the value of the ath and $(a + 1)$th members. We want the value (in the units of the variable) for the given p. Let this be $\underline{p}$. Then

$$\underline{p} = \underline{a} + [np - (a - 0.5)][\underline{(a+1)} - \underline{a}].$$

We define the G span as that distance which, were the sample or population distributed in a Gaussian ("normal") fashion, would give the same numerical value as the standard deviation. Specifically, G span = $\underline{p}_{0.69} - \underline{p}_{0.31}$.

Appendix B: Details of the Simulation

B1. Physical Conditions

The model comprised 66 layers representing a horizontal slice through the container and its contents plus a computational sentinel layer at top and bottom. The saturated and unsaturated zone layers were 0.5 cm thick; the headspace had a 9 cm layer sandwiched between two 0.5 cm layers; the lid of the container was 0.3 cm thick (and the area of the headspace sidewalls was added to it). The headspace was entirely gas phase. The saturated and unsaturated zones were assumed to contain organic matter at a dry bulk density of 0.05 g cm^{-3} and of intrinsic density 1.5 g cm^{-3}, so a proportion 0.05/1.5 = 0.033 (just over 3%) of the space in these layers was occupied by solid matter. Most of this solid matter is in almost unhumified macroscopic pieces, so it was assumed to be physically, but not biologically, inert and without direct influence on transfer processes. In the unsaturated zone the associated water probably does influence transport, so it must be included in the simulation. Most of the solid matter is *Sphagnum* cell walls, which present little resistance to diffusion: in effect the tortuosity is small. This contrasts with mineral soils in which most of the solid matter is in small impermeable pieces causing large tortuosity and kinetics dominated by bottlenecks.

The saturated zone contained organic matter and water only: measurements of wet mass and dry mass on slices of accurately known volume from cores similar to the experimental one [*Clymo*, 1983, 1984, 1992, unpublished manuscript, 1995] show no sign of an extensive gas phase below the water table. Nor did vertical probes attached directly to a mass spectrometer: gas bubbles manifest themselves by a large increase in partial pressure (W. Daulat, unpublished manuscript, 1995). We do not deny that gas bubbles may be found in the peat below pools (for example), but we think they were unimportant in this experiment so we made no attempt to simulate them or their movement.

In the unsaturated zone the proportion of the void volume occupied by water, p_W was given by $p_W = 10^{(x/L - 1)}$, where x is the distance down into the unsaturated zone and L is its total thickness. This function is a negative exponential from 10% of the void volume occupied by water at the top of the top layer to 100% at the bottom of the lowermost unsaturated layer. This approximates experimental measurements [*Clymo*, 1983, 1984, 1992, unpublished, 1995].

B2. Processes

Mass transfers were made first and were simply sums of rates in and out multiplied by the time step. After mass transfers, the total gas in the unsaturated layers was redistributed between gas and

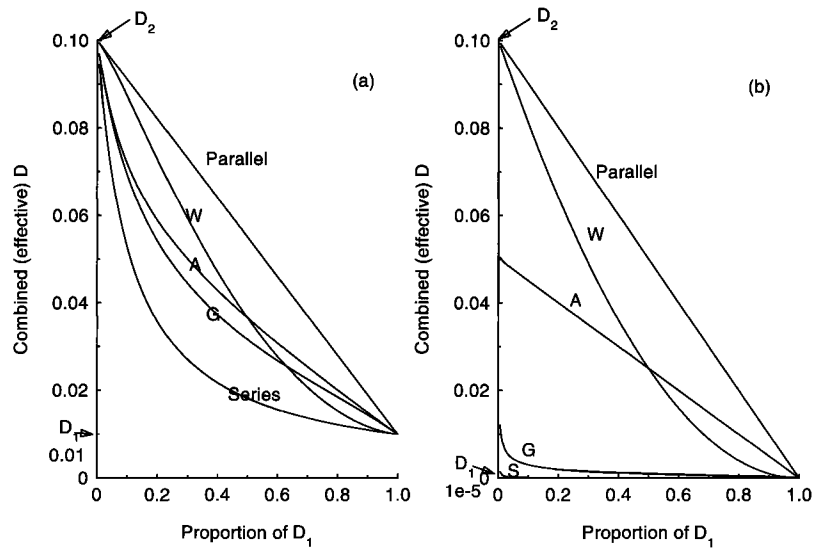

Figure 8. Effective transfer coefficient (D) as a function of the proportion of materials with two different values of D combined in various ways. (a) $D_2 = 0.1$, $D_1 = 0.01$. The lowest curve is for layers of the two materials in series, and the highest curve is for the two materials in parallel (see text and appendix B). Also shown are curves for the combination of series and parallel: A indicates arithmetic mean; G indicates geometric mean; and W indicates mean weighted by the proportion (see appendix B). All the curves coincide at the two points 0, D_2 and 1, D_1. The choice of D_2, with units $cm^2\ s^{-1}$, is appropriate for air. D_1 was chosen to show the shapes of the curves. (b) D_2 as in Figure 8a, $D_1 = 1.0 \times 10^{-5}$, appropriate for diffusion of gases in water. With large differences in the D values, the curves become very different from each other.

water phases using the solubility coefficients for 20°C: Kr, 0.067; CH_4, 0.033; and CO_2, 0.880 $cm^3\ cm^{-3}$.

Nine rates were calculated. Five were fluxes described formally by $\Delta M/\Delta t = D\ A\ \Delta C/\Delta x$, where M is mass, t is time, C is concentration, x is distance, and D is a transfer coefficient. These five fluxes were of Kr, $^{12}CH_4$, $^{12}CO_2$, $^{13}CH_4$, and $^{13}CO_2$ between adjacent layers. We used one value of D for all gases in the gas phase and a second value for all gases in water.

There were complications in the unsaturated layers: the overall (effective) transfer coefficient depends on how the gas and water are arranged. If a half-thickness layer of one follows a half-thickness layer of the other in either order (series arrangement), then the conductance is low: only double what it would be if the whole layer were of low-conductance material. If, however, the two materials are in parallel, then the overall conductance is high: only half that if the whole layer was of high-conductance material.

Let D_1 and D_2 be the conductivity of the two substances that are in proportions P_1 and P_2, with $P_T = P_1 + P_2$, then D_S and D_P, the effective series and parallel conductivity, are

$$D_S = P_T/(P_1/D_1 + P_2/D_2)$$

$$D_P = (P_1D_1 + P_2D_2)/P_T.$$

Figure 8 shows the effective conductivity of differing proportions of the two materials: in series at the bottom and (the topmost sloping straight line) in parallel. Figure 8 also shows the effects of taking a simple arithmetic or geometric average of the two values of D.

The parallel arrangement is not wholly realistic, even though many of the structural elements in the unsaturated layer, and their associated water, do run vertically. The effective conductivity is too great (except at the ends of the proportion scale). The series and simple average are wildly unsatisfactory giving as they do little increase in effective conductivity until the proportion of the low conductivity material has become very small, when there is a very large increase. We therefore used a weighted effective mean defined by

$$D_e = (P_1D_S + P_2D_P)/P_T,$$

where $D_1 < D_2$. As Figure 8 shows, when the layer is mostly unsaturated (the proportion of D_1 is small), the layer behaves close to parallel, but by the time the proportion of D_1 is 90% and the layer is mostly saturated, it behaves close to the series arrangement.

These rate calculations required three parameters: the transfer coefficients in the gas phase, in water, and in the container lid and headspace walls, D_g, D_w, and D_c.

Two of the other four rates concerned the generation of natural CH_4 and CO_2 by decay. We assumed, for simplicity, that all the CO_2 was generated in the unsaturated layers at a rate proportional to the mass in the layer. The CH_4 was assumed to be generated in a layer 3 cm thick 10 cm below the top of the topmost saturated layer, consistent with measurements [*Daulat and Clymo*, 1998, unpublished manuscript, 1996]. The decay processes required one parameter each for CH_4 and CO_2: P_M and P_C.

The remaining two rates were of the oxidation of CH_4 to CO_2 for ^{12}C and excess ^{13}C, which we supposed to follow the same hyperbolic relation between rate and concentration of CH_4 in water. This required two more parameters: H_V representing the maximum rate when concentration is not limiting and H_K the concentration for half-maximal rate. The oxidation process was restricted to the unsaturated layers: *Nedwell and Watson* [1995] reported that CH_4 oxidation at Ellergower Moss was entirely aerobic, though anaerobic oxidation is known to be possible [e.g., *Alperin and Reeburgh*, 1985].

B3. Running the Simulation

The method used is outlined in the main text. At the start of a run, all concentrations were set to zero, and there was no Kr or excess ^{13}C anywhere. The model was then run for 10^4 min, with increments of 0.2 min, or until no layer showed more than 0.05% change from the previous iteration in concentration of any gas. This established the initial gas concentration profiles. The water in the top 1.5 cm of the saturated layers was then notionally removed and replaced by water saturated with Kr and $^{13}CH_4$, and the run resumed.

In early runs we set the time increment to 5 min, but the behavior was unstable with alternate layers building up increasing and reversing oscillations in concentration. We cured this by two actions. First we calculated full mass changes, but then implemented only half the full change plus the half change left over from the previous iteration. This is similar to the partial explicit, partial implicit technique used in finite difference hydrological modeling. Second we made the time increment very short (0.2 min) and increased it cautiously only if no concentration was more than 1% different from its value on the previous iteration. If this limit was exceeded for any difference in any layer, the time increment was substantially reduced. These approaches required far more computing time (a single run took more than an hour on a 100 MHz machine), but the results were stable.

The criterion to be minimized was similar to a chi-square quantity: $\Sigma[(y_{\mathrm{obs},j} - y_{\mathrm{calc},j}) / y_{GS,j}]^2$, where the sum is over all sample times and $j = 1 \ldots 5$ gases, $y_{\mathrm{obs},j}$ is the measured value of the jth gas in the headspace at time t, $y_{\mathrm{calc},j}$ is the corresponding value calculated in the model, and $y_{GS,j}$, an inverse weight, is the measurement error of $y_{\mathrm{obs},j}$ assessed by the G span. We applied a further weight to each quantity in the sum because observations were far more frequent in the early part of the experiment. This weight was the logarithm of the time into the experiment, standardized so that the mean weight was 1.0. We also applied a third weight that was the inverse of the mean proportional error for each gas, standardized to a mean weight of 1.0. The values for the five gases ranged from 0.4 to 2.1. This weighting was to make the importance proportional to the precision of measurement for the different gases.

We optimized the parameter values (minimized the criterion) by the method of *Nelder and Mead* [1965]. This is a simple and robust method, though not the fastest. The model and optimization were programmed in PASCAL.

Acknowledgments. We thank P. Cook for making the mass spectrometer measurements, four reviewers for comments on drafts of the article, and the Natural Environment Research Council for financial support. Both authors designed the work; D. M. E. P. made the experiments; R. S. C. undertook data reduction, model building, and the first draft of this article.

References

Alm, J., *CO_2 and CH_4 Fluxes and Carbon Balance in the Atmospheric Interaction of Boreal Peatlands*, Ph.D. thesis, Publ. in Sci. 44, Univ. of Joensuu, Joensuu, Finland, 1997.

Alperin, M. J., and W. S. Reeburgh, Inhibition experiments on anaerobic methane oxidation, *Appl. Environ. Microbiol.*, *50*, 940–945, 1985.

Andersen, B. L., G. Bidoglio, A. Leip, and D. Rembges, A new method to study simultaneous methane oxidation and methane production in soils, *Global Biogeochem. Cycles*, *12*, 587–594, 1998.

Bartlett, K. B., and R. C. Harriss, Review and assessment of methane emissions from wetlands, *Chemosphere*, *26*, 261–320, 1993.

Belyea, L. R., Separating the effects of litter quality and microenvironment on decomposition rates in a petterned peatland, *Oikos*, *77*, 529–539, 1996.

Belyea, L. R., and R. S. Clymo, Do hollows control the rate of peat bog growth?, in *Patterned Mires and Mire Pools*, edited by V. Standen, J. H. Tallis, and R. Meade, pp. 55–65, British Ecol. Soc., London, 1998.

Bircumshaw, L. L., and A. C. Riddiford, Transport control in heterogeneous reactions, *Quart. Rev.*, *6*, 157–185, 1952.

Briggs, G. E., A. B. Hope, and R. N. Robertson, *Electrolytes and Plant Cells*, 216 pp., Blackwell Sci., Malden, Mass., 1961.

Brumme, R., and W. Borken, Site variation in methane oxidation as affected by atmospheric deposition and type of temperate forest ecosystem, *Global Biogeochem. Cycles*, *13*, 493–501, 1999.

Chanton, J. P., J. E. Bauer, P. A. Glaser, D. I. Siegel, C. A. Kelley, S. C. Tyler, E. H. Romanowicz, and A. Lazrus, Radiocarbon evidence for the substrates supporting methane formation within northern Minnesota peatlands, *Geochim. Cosmochim. Acta*, *59*, 3663–3668, 1995.

Clymo, R. S., Peat, in *Ecosystems of the World, vol. 4A, Mires: Swamp, Bog, Fen and Moor*, edited by A. J. P. Gore, pp. 159–224, Elsevier, New York, 1983.

Clymo, R. S., The limits to peat bog growth, *Philos. Trans. R. Soc. London, Ser. B*, *303*, 605–654, 1984.

Clymo, R. S., Models of peat growth, *Suo*, *43*, 127–136, 1992.

Clymo, R. S., *Sphagnum*, the peatland carbon economy, and climate change, in *Bryology for the Twenty First Century*, edited by J. W. Bates, N. W. Ashton, and J. G. Duckett, pp. 361–368, J. G. Maney, Leeds, U.K., 1998.

Clymo, R. S., and D. M. E. Pearce, Methane and carbon dioxide production in, transport through, and efflux from a peatland, *Philos. Trans. R. Soc. London, Ser. A*, *350*, 249–259, 1995.

Clymo, R. S., and E. J. F. Reddaway, Productivity of *Sphagnum* (bog-moss) and peat accumulation, *Hydrobiologia*, *12*, 181–192, 1971.

Clymo, R. S., J. Turunen, and K. Tolonen, Carbon accumulation in peatland, *Oikos*, *81*, 368–388, 1998.

Conrad, R., Soil microorganisms as controllers of atmospheric trace gases (H_2, CO, CH_4, OCS, N_2O, and NO), *Microbiol. Rev.*, *60*, 609–640, 1996.

Crill, P. M., Seasonal patterns of methane uptake and carbon dioxide release by a temperate woodland soil, *Global Biogeochem. Cycles*, *5*, 319–334, 1991.

Crill, P. M., K. Bartlett, and N. Roulet, Methane flux from Boreal peatlands, *Suo*, *43*, 173–182, 1993.

Crill, P. M., P. J. Martikainen, H. Nykänen, and J. Silvola, Temperature and N fertilization effects on methane oxidation in a drained peatland soil, *Soil Biol. Biochem.*, *26*, 1331–1339, 1994.

Daulat, W. E., and R. S. Clymo, Effects of temperature and water table on the efflux of methane from peatland surface cores, *Atmos. Environ.*, *32*, 3207–3218, 1998.

Dunfield, P., R. Knowles, R. Dumont, and T. R. Moore, Methane production and consumption in temperate and sub-arctic peat soils: Response to temperature and pH, *Soil Biol. Biochem.*, *25*, 321–326, 1993.

Fechner, E., and H. Hemond, Methane transport and oxidation in the unsaturated zone of a *Sphagnum* peatland, *Global Biogeochem. Cycles*, *6*, 33–44, 1992.

Gorham, E., Northern peatlands: Role in the carbon cycle and probable responses to climatic warming, *Ecol. Appl.*, *1*, 182–195, 1991.

Gulledge, J., and J. P. Schimel, Low-concentration kinetics of atmospheric CH_4 oxidation in soil and mechanism of NH_4^+ inhibition, *Appl. Environ. Microbiol.*, *64*, 4291–4298, 1998.

Houghton, J. T., L. G. Meira Filho, B. A. Callander, N. Harris, A. Kattenberg, and K. Maskell (Eds.), *Climate Change 1995*, 564 pp., Cambridge Univ. Press, New York, 1996.

Ingram, H. A. P., Soil layers in mires: function and terminology, *J. Soil Sci.*, *29*, 224–227, 1978.

Iversen, N., R. S. Ormeland, and M. J. Klug, Big Soda Lake (Nevada), 3, Pelagic methanogenesis and anaerobic methane oxidation, *Limnol. Oceanogr.*, *32*, 804–814, 1987.

King, G. M., and A. P. S. Adamsen, Effects of temperature on methane consumption in a forest soil and in pure cultures of the methanotroph *Methylomonas rubra*, *Appl. Environ. Microbiol.*, *58*, 2758–2763, 1992.

Malmer, N., B. M. Svensson, and B. Wallén, Interactions between *Sphagnum* mosses and vascular plants in the development of peat forming systems, *Folia Geobotanica et Phytotaxonomica*, *29*, 483–496, 1994.

Nedwell, D. B., and A. Watson, CH_4 production, oxidation and emission in a U.K. ombrotrophic peat bog: influence of SO_4^{2-} from acid rain, *Soil Biol. Biochem.*, *27*, 893–903, 1995.

Nelder, J. A., and R. Mead, A simplex method for function minimization, *Comp. J.*, *7*, 308–313, 1965.

Olsen, C., The significance of concentration for the rate of ion absorption by higher plants in water culture, II, Experiments with aquatic plants, *Physiol. Plant.*, *6*, 837–843, 1953a.

Olsen, C., The significance of concentration for the rate of ion absorption by higher plants in water culture, III, The importance of stirring, *Physiol. Plant.*, *6*, 844–847, 1953b.

Ormeland, R. S., and D. C. Capone, Use of "specific" inhibitors in biogeochemistry and microbial ecology, *Adv. Microbiol.*, *10*, 285–383, 1988.

Reeburgh, W. S., B. B. Ward, S. C. Whalen, A. Sandbeck, K. K. Kilpatrick, and L. J. Kerkhof, Black Sea methane geochemistry, *Deep Sea Res.*, *Part A*, *38*, S1189–S1210.3, 1991.

Reeburgh, W. S., S. C. Whalen, and M. J. Alperin, The role of methylotrophy in the global methane budget, in *Microbial Growth on C_1 Compounds*, edited by J. C. Murrell and D. P. Kelly, pp. 1–14, Intercept, Andover, Hants, U. K., 1993.

Reeburgh, W. S., A. I. Hirsch, F. J. Sansone, B. N. Popp, and T. M. Rust, Carbon isotope effect accompanying microbial oxidation of methane in Boreal forest soils, *Geochim. Cosmochim. Acta*, *61*, 4761–4767, 1997.

Rivers, J. S., D. I. Siegel, L. S. Chasar, J. P. Chanton, P. A. Glaser, N. T. Roulet, and J. M. McKenzie, A stochastic appraisal of the annual carbon budget of a large circumboreal peatland, Rapid River Watershed, northern Minnesota, *Global Biogeochem. Cycles*, *12*, 715–727, 1998.

Saarnio, S., J. Alm, P. J. Martikainen, and J. Silvola, Effects of raised CO_2 on potential CH_4 production and oxidation in, and CH_4 emission from, a boreal mire, *J. Ecol.*, *86*, 261–268, 1998.

Sundh, I., C. Mikkelä, M. Nilsson, and B. Svensson, Potential methane oxidation in a *Sphagnum* peat bog: Relation to water table level and vegetation type, in *Proceedings of the 9th International Peat Congress, Uppsala 1992, vol. 3*, pp. 142–151, Int. Peat Soc., Jyväskylä, Finland, 1992.

Sundh, I., M. Nilsson, and B. H. Svensson, Depth distribution of methane production and oxidation in a *Sphagnum* peat bog, *Suo*, *43*, 267–269, 1993.

Sundh, I., M. Nilsson, G. Granberg, and B. H. Svensson, Depth distribution of microbial production and oxidation of methane in northern Boreal peatlands, *Microbial Ecol.*, *27*, 253–265, 1994.

Sundh, I., P. Borgå, M. Nilsson, and B. H. Svensson, Estimation of cell numbers of methanotrophic bacteria in Boreal peatlands based on analysis of specific phospholipid fatty acids, *FEMS Microbiol. Ecol.*, *18*, 103–112, 1995.

Whalen, S. C., and W. S. Reeburgh, Consumption of atmospheric methane by tundra soils, *Nature*, *346*, 160–162, 1990.

Whalen, S. C., W. S. Reeburgh, and K. A. Sandbeck, Rapid oxidation in landfill cover soil, *Appl. Environ. Microbiol.*, *56*, 3405–3411, 1990.

Whalen, S. C., W. S. Reeburgh, and K. S. Kizer, Methane consumption and emission by taiga, *Global Biogeochem. Cycles*, *5*, 261–273, 1991.

Whalen, S. C., W. S. Reeburgh, and V. A. Barber, Oxidation of methane in Boreal forest soils: A comparison of seven measures, *Biogeochemistry*, *16*, 181–211, 1992.

Yavitt, J. B., G. G. Lang, and D. M. Downey, Potential methane production and methane oxidation rates in peatland ecosystems of the Appalachian Mountains, United States, *Global Biogeochem. Cycles*, *2*, 253–268, 1988.

Yavitt, J. B., D. M. Downey, E. Lancaster, and G. G. Lang, Methane consumption in decomposing *Sphagnum*-derived peat, *Soil Biol. Biochem.*, *22*, 441–447, 1990.

R. S. Clymo, School of Biological Sciences, Queen Mary, University of London, London, E1 4NS, U.K.

D. M. E. Pearce, School of Biological and Molecular Sciences, Oxford Brookes University, Gipsy Lane Campus, Headington, Oxford, OX3 0BP U.K. (dpearce@brookes.ac.uk)

(Received July 3, 2000; revised December 4, 2000;
accepted December 29, 2000.)